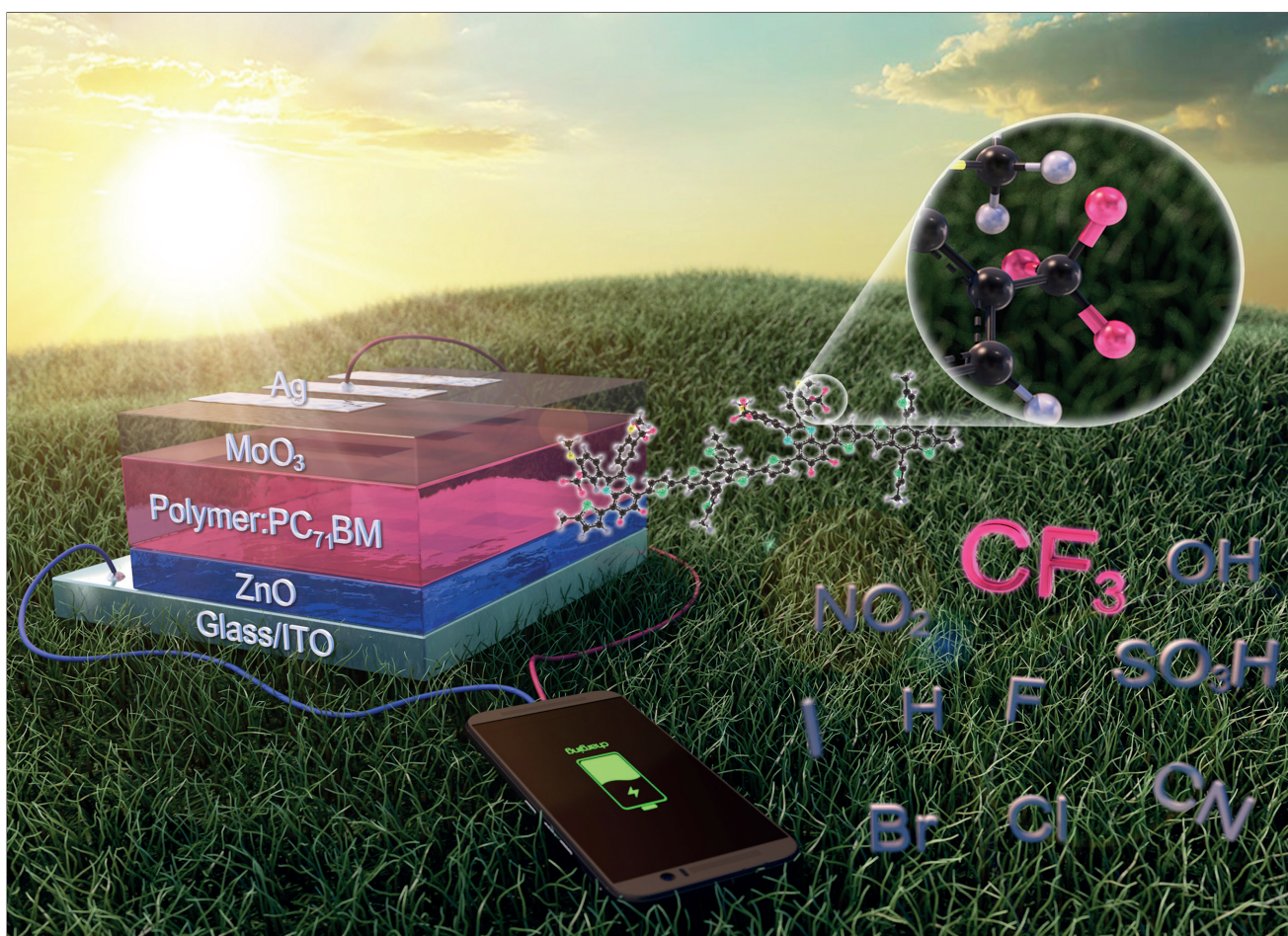




Macromolecular Rapid Communications



16/2018

WILEY-VCH



Synthesis of Trifluoromethylated Quinoxaline-Based Polymers for Photovoltaic Applications

Sella Kurnia Putri, Yun Hwan Kim, Dong Ryeol Whang, Joo Hyun Kim,*
and Dong Wook Chang*

A series of quinoxaline-based conjugated polymers, in which the electron-donating benzodithiophene (BDT) unit is linked to the electron-accepting 6,7-difluorinated quinoxaline (DFQ) derivatives by a thiophene bridge, is synthesized. To investigate their effects on the intrinsic properties of polymers, strong electron-withdrawing trifluoromethyl (CF₃) groups were incorporated into the meta-position of the phenyl ring at the 2,3-positions of the DFQ unit of the reference polymer, labelled PEhB-FQx, to yield the target polymer PEhB-FQxCF₃. In addition, the 2-ethylhexyloxy substituents on the BDT donor in PEhB-FQxCF₃ are changed to the more planar 2-ethylhexyl thiophene units to produce another target polymer PThB-FQxCF₃. Owing to the significant contributions of the CF₃ moiety, PEhB-FQxCF₃ exhibits quite discernible optical and electrochemical properties along with significant enhancement in photovoltaic performances compared to the reference polymer PEhB-FQx. Furthermore, the incorporation of the alkylthienyl side chains on the BDT moiety confers on the resultant PThB-FQxCF₃ to possess the maximum power conversion efficiency of 7.26% with an open circuit voltage of 0.88 V, short-circuit current density of 12.20 mA cm⁻², and fill factor of 67.80%.

The unique advantages of polymer solar cells (PSCs) such as cost-effectiveness, lightweight, ease of processability, and outstanding flexibility, render them promising next generation solar energy conversion devices.^[1,2] Continuous innovation in material synthesis and device fabrication has greatly improved the power conversion efficiencies (PCEs) of PSCs to more than 10%.^[3-6] Bulk heterojunction structures between organic semiconductor-

based electron-donors and fullerene-based electron-acceptors are usually preferred for the construction of an efficient active layer. Therefore, a wide range of conjugated polymeric donors with alternating electron-donating (D) and electron-accepting (A) units along their backbones has been intensively developed for high-performance PSCs.^[7] Significant reduction in their bandgaps can be achieved simply by efficient formation of the intramolecular charge transfer (ICT) state in these D–A configuration. The appropriate combination of D and A constituents is also of great importance to determine the intrinsic properties of the D–A polymer including energy levels, optical absorption, and carrier mobility.^[8] In particular, quinoxaline (Qx) has attracted tremendous interest as an electron-withdrawing moiety for constructing low-bandgap polymers, because of its favorable characteristics such as strong electron affinity, ease of preparation, and high structural versatility.^[9,10]

Recently, the introduction of electron-withdrawing substituents like fluorine (F) atom into the structure of low bandgap polymers has been regarded as one of the promising strategies for improving the photovoltaic properties of PSCs.^[11-13] Compared with their nonfluorinated counterparts, fluorinated polymers exhibit low-lying energy levels in both the lowest unoccupied molecular orbital (LUMO) and highest occupied molecular orbital (HOMO) without serious interruption in bandgap. Therefore, higher values of open circuit voltage (V_{oc}) as well as enhanced PCEs can usually be achieved from PSCs with fluorinated polymers. It has been also reported that the electronic and photovoltaic properties of Qx-based low-bandgap polymers are strongly dependent on the position and number of F atoms in their skeleton.^[14] In addition, tetrafluoroquinoxaline- and hexafluoroquinoxaline-based polymers exhibit excellent PCEs of 9.12% and 9.40%, respectively, in the presence of nonfullerene acceptors.^[15,16] The recent pioneering study on constructing fluorinated quinoxaline-based polymers could enhance their PCEs up to 11.3% in a fullerene-free organic solar cell.^[17]

Apart from the F atom, other strong electron-withdrawing moieties such as sulfonyl (SO₂), trifluoromethyl (CF₃), and cyano (CN) can be incorporated into the structure of conjugated polymers to achieve noticeable improvements in

S. K. Putri, Prof. D. W. Chang
Department of Industrial Chemistry
Pukyong National University
Pusan 48547, Republic of Korea
E-mail: dwchang@pknu.ac.kr

Y. H. Kim, Prof. J. H. Kim
Department of Polymer Engineering
Pukyong National University
Pusan 48547, Republic of Korea
E-mail: jkim@pknu.ac.kr

Prof. D. R. Whang
Linz Institute for Organic Solar Cells/Institute of Physical Chemistry
Johannes Kepler University
Linz 4040, Austria

The ORCID identification number(s) for the author(s) of this article can be found under <https://doi.org/10.1002/marc.201800260>.

DOI: 10.1002/marc.201800260

the photovoltaic properties of PSCs.^[18–20] In particular, the CF₃ group has received considerable interest, because it not only possesses higher electron-withdrawing capability than the F atom but also enables facile tuning of important properties including chemical stability, thermal stability, and solubility.^[21,22] The electronic contributions of the substituents can be expressed by their Hammett constants (σ); the corresponding values for CF₃ and F on the *meta*-position (σ_p) of benzene were calculated as 0.43 and 0.34, respectively.^[21] The stronger electron-withdrawing capability of CF₃ unit can make it more favorable for lowering HOMO energy levels of conjugated polymers than F atom. Moreover, the existence of multiple F atoms in CF₃ unit can efficiently trigger intermolecular or intramolecular aggregation in solid state through the strengthened F–F and F–H interactions. So it can be deduced that trifluoromethylated polymers are quite useful for the development of high performance PSCs with enhanced V_{oc} and J_{sc} . Zhang et al. reported that CF₃ groups on the electron-donating triphenylamine moiety in a D–A polymer can increase the V_{oc} of the PSC up to 1.00 V.^[23] In addition, several D–A polymers with CF₃ groups on the electron-withdrawing components have been prepared for photovoltaic applications.^[19,22,24] However, the PCEs of these CF₃-containing D–A type polymers have remained less than 1.5% so far. Therefore, more systematic studies are required to develop high-performance polymers with strong electron-withdrawing CF₃ components for photovoltaic applications.

In this article, a series of Qx-based low-bandgap polymers with a typical D–A configuration were synthesized by the Stille coupling reaction, in which the electron-donating benzodithiophene (BDT) monomers were linked to the electron-withdrawing 6,7-difluorinated quinoxaline (DFQ) derivatives through a thiophene bridge. At first, 2,6-bis(trimethyltin)-4,8-bis(2-ethylhexyloxy)benzo[1,2-*b*:4,5-*b'*]dithiophene and 5,8-bis(5-bromothiophen-2-yl)-2,3-bis(4-(2-ethylhexyloxy)phenyl)-6,7-difluoroquinoxaline were polymerized to synthesize the reference polymer PEhB-FQx. Next, two CF₃ moieties were incorporated on to the *meta*-position of the phenyl ring at the 2,3-positions of DFQ in the structure of PEhB-FQx to afford PEhB-FQxCF₃. This specific location of the newly introduced CF₃ moieties in PEhB-FQxCF₃ has been known to be a promising position for the introduction of electron-withdrawing constituents to prepare high-performance Qx-based polymers for PSCs.^[15,25] Finally, while maintaining the

strong electron-withdrawing CF₃ moiety on the DFQ unit, the 2-ethylhexyloxy substituted groups on the BDT monomer were replaced with 2-ethylhexyl thiophene to prepare PThB-FQxCF₃. The chemical structures of all the polymers are shown in **Figure 1**. Owing to the significant contributions of the electron-accepting CF₃ moieties, the polymer PEhB-FQxCF₃ exhibited quite discernible optical and electrochemical properties along with significant enhancement in photovoltaic performances compared with PEhB-FQx. Furthermore, the promotion of intermolecular coplanarity by introducing alkylthienyl groups on the BDT unit can further enhance PCE to as much as 7.26% in PThB-FQxCF₃-based devices.

The synthetic routes for the monomers and polymers are outlined in **Scheme 1**. For the synthesis of monomers, α -diketone with two electron-withdrawing CF₃ groups at the *meta*-position of benzene (**3**) was first prepared by a two-step process of consecutive reactions: alkylation of 4-bromo-2-(trifluoromethyl)phenol (**1**) to afford 4-Bromo-1-(2-ethylhexyloxy)-2-(trifluoromethyl)benzene (**2**), and the formation of α -diketone (**3**) using **2** and dimethylpiperazine-2,3-dione as reactants. The CF₃-containing DFQ derivative (**4**) was produced by zinc (Zn)-mediated reduction of 5,6-difluoro-4,7-di(thiophen-2-yl)-benzo[*c*][1,2,5]thiadiazole followed by condensation with the related α -diketone (**3**). Finally, bromination of **3** with *N*-bromosuccinimide (NBS) can produce the dibrominated CF₃-containing DFQ-based monomer of **5**. Besides, other monomers such as 2,6-bis(trimethyltin)-4,8-bis(2-ethylhexyloxy)benzo[1,2-*b*:4,5-*b'*]dithiophene (**6**), 2,6-bis(trimethyltin)-4,8-bis(5-(2-ethylhexyl)thiophen-2-yl)benzo[1,2-*b*:4,5-*b'*]dithiophene (**7**), and 5,8-bis(5-bromothiophen-2-yl)-2,3-bis(4-(2-ethylhexyloxy)phenyl)-6,7-difluoroquinoxaline (**8**) were synthesized according to the literature.^[26–28] The systematic combination of the electron-donating BDT monomers and electron-withdrawing DFQ monomers such as **6** and **8**, **6** and **5**, and **7** and **5**, can produce three discernible polymers, that is, PEhB-FQx, PEhB-FQxCF₃, and PThB-FQxCF₃, respectively, under Stille polycondensation conditions. These polymers dissolve well in common organic solvents such as chloroform, tetrahydrofuran, and toluene, due to the presence of multiple 2-ethylhexyloxy side chains on the BDT as well as DFQ units. The weight average molecular weights (M_w) of PEhB-FQx, PEhB-FQxCF₃, and PThB-FQxCF₃, as measured by gel permeation chromatography, are 24.06, 98.64, and 84.77 KDa, respectively, with polydispersity indexes (PDI) of 2.49, 1.90, and 2.24, respectively. In addition,

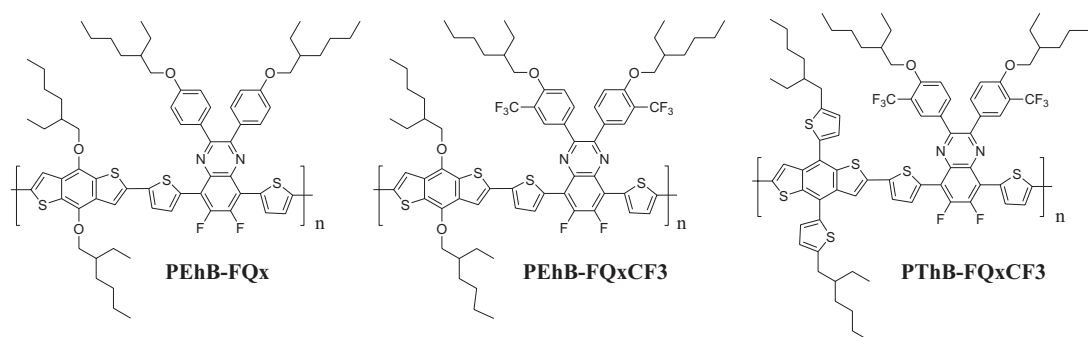
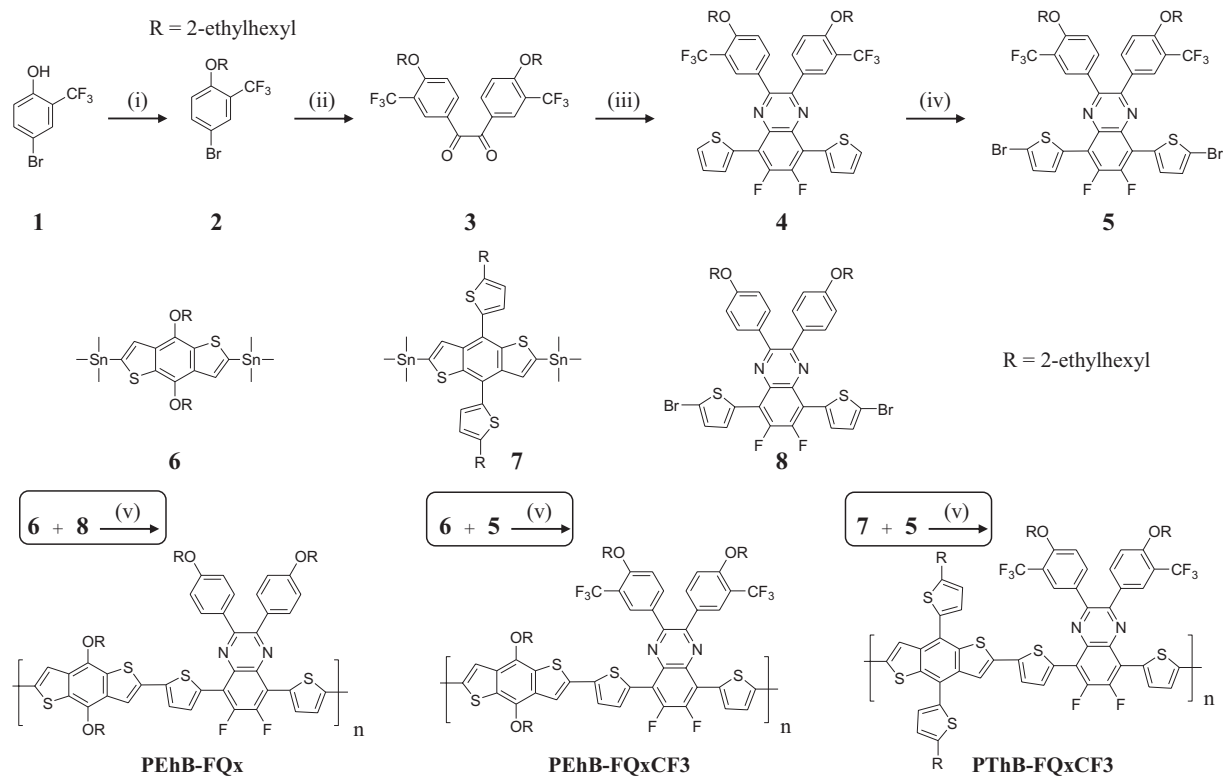


Figure 1. Chemical structures of PEhB-FQx, PEhB-FQxCF₃, and PThB-FQxCF₃.



Scheme 1. Synthetic routes for monomers and polymers: i) 2-ethylhexyl bromide, K_2CO_3 , at 100 °C overnight; ii) *n*-butyllithium/tetrahydrofuran (*n*-BuLi/THF), at –78 °C for 1 h; then 1,4-dimethylpiperazine-2,3-dione, at room temperature (RT) overnight; iii) 5,6-difluoro-4,7-di(thiophen-2-yl)-benzo[*c*][1,2,5]thiadiazole, zinc (Zn)/acetic acid, at 100 °C for 12 h; then α -diketone/acetic acid, reflux for 12 h; iv) *N*-bromosuccinimide (NBS), RT overnight, and v) tetrakis(triphenylphosphine)palladium(0) ($Pd(PPh_3)_4$), at 90 °C for 48 h.

all polymers exhibited good thermal stability, and similar values of decomposition temperatures at 5% weight loss ($T_{d5\%}$) of over 335 °C (Figure S1, Supporting Information).

The polymer films exhibit two broad UV-Vis absorption bands (Figure 2a) at 350–450 nm and 500–650 nm, respectively. The former corresponds to the localized π – π^* transition of the polymer backbone, and the latter relates to ICT between the D and A units in the polymer backbone. This is characteristic of polymers with D–A configuration. The absorption band in the longer wavelength region and the band gap of PEhB-FQxCF3 are 590 nm and 1.74 eV, respectively, which are slightly

blue-shifted than those of PEhB-FQx (596 nm and 1.75 eV). This is possibly due to the presence of the electron-withdrawing CF_3 groups on the DFQ unit.^[14] On the other hand, the absorption band in the longer wavelength region of PThB-FQxCF3 appears to be red-shifted at 600 nm. Similar trends in the UV-Vis absorption spectra were observed when PTB7 and PTB7-Th were compared.^[29] This shift is due to the higher effective conjugation length of PThB-FQxCF3 upon incorporation of the more planar alkylthienyl moiety on the BDT unit. However, the optical band gap of PThB-FQxCF3 is calculated to be 1.75 eV, which is almost identical to that of PEhB-FQx.

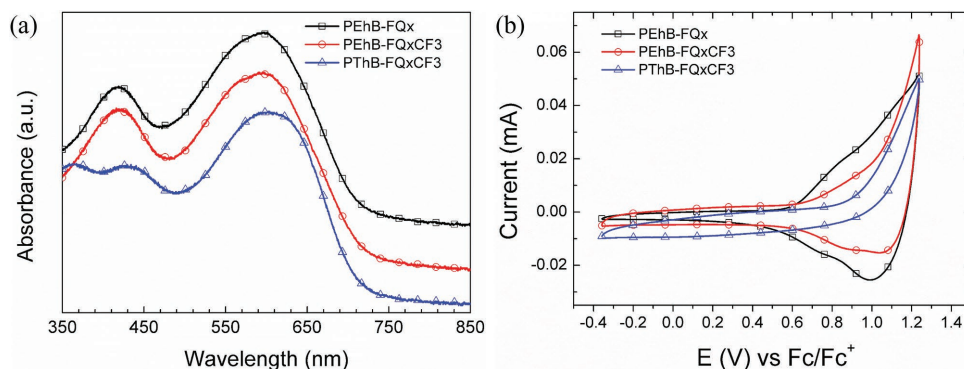


Figure 2. a) UV-Vis spectra of polymer films (spectra are offset for clarity), and b) cyclic voltammograms of PEhB-FQx, PEhB-FQxCF3, and PThB-FQxCF3.

Table 1. Summary of optical and electrochemical properties of polymers.

Polymer	λ_{edge} [nm] ^{a)}	$E_{\text{gap}}^{\text{opt}}$ [eV] ^{b)}	λ_{max} [nm] ^{c)}	HOMO [eV] ^{d)}	LUMO [eV] ^{e)}
PEhB-FQx	709, 1.75		418, 596	-5.35	-3.61
PEhB-FQxCF ₃	713, 1.74		418, 590	-5.42	-3.68
PThB-FQxCF ₃	709, 1.75		426, 600	-5.58	-3.81

^{a)}Absorption edge of the film; ^{b)}Estimated optical bandgap from λ_{edge} ; ^{c)}Maximum wavelength of the film; ^{d)}Obtained from the oxidation onset potential; ^{e)}Calculated from the optical bandgap and the HOMO energy level.

The HOMO energy levels of PEhB-FQx, PEhB-FQxCF₃, and PThB-FQxCF₃ calculated from the oxidation onset potential of the cyclic voltammograms (CVs) (Figure 2b) were -5.35, -5.42, and -5.58 eV, respectively. It is noteworthy that the incorporation of the CF₃ moieties renders the HOMO level of PEhB-FQxCF₃ (-5.42 eV) lower than that of PEhB-FQx (-5.35 eV). The HOMO level of PThB-FQxCF₃ is even lower at -5.58 eV due to the introduction of alkylthienyl side chains into the structure of the BDT unit. The LUMO energy levels of PEhB-FQx, PEhB-FQxCF₃, and PThB-FQxCF₃ can be determined from their HOMO energy levels and the optical bandgap, and the values are -3.61, -3.68, and -3.81 eV, respectively. The optical and electrochemical properties of the polymers are summarized in Table 1. The results obtained from the UV-Vis and CV analyses demonstrate the significant contributions of the strong electron-withdrawing CF₃ groups of the DFQ moiety as well as alkylthienyl substituents of the BDT unit to the energy levels of the CF₃-modified DFQ-based polymers.

The electronic structures and the frontier molecular orbitals of PEhB-FQx, PEhB-FQxCF₃, and PThB-FQxCF₃ were determined using the density functional theory at the B3LP/6-31G** level of the Gaussian 09 program.^[30] All the side chains on the BDT donor and DFQ acceptor are abbreviated to methyl groups, and long polymer chains are reduced to two repeating units for computational simplicity. As shown in Figure S2, Supporting Information, the HOMO wave functions of the polymers are delocalized along their backbones, while the LUMO wave functions are highly localized in the electron-withdrawing DFQ units. Moreover, upon incorporation of the strong electron-withdrawing CF₃ components, stronger charge transfer characteristics are observed in PEhB-FQxCF₃ and PThB-FQxCF₃ than in PEhB-FQx.

To elucidate the photovoltaic properties of the polymers, inverted type PSCs were fabricated with the structure of indium tin oxide (ITO)/ZnO(25 nm)/active layer(polymer:PC₇₁BM) (80 nm)/MoO₃(20 nm)/Ag(100 nm). The electronic energy level of the polymers and other materials used in the construction of the PSCs are illustrated in Figure 3a. Based on the energy level diagrams, efficient charge separation from the polymer to PC₇₁BM, and charge carrier transport in the PSCs can be expected. Several different blend ratios of the polymer and PC₇₁BM ranging from 3:2 to 3:5 w/w in the active layer were tested, and the optimum blend ratios of PEhB-FQx, PEhB-FQxCF₃, and PThB-FQxCF₃, to PC₇₁BM were determined to be 3:3, 3:4, and 3:4, respectively (Table S1, Supporting Information).

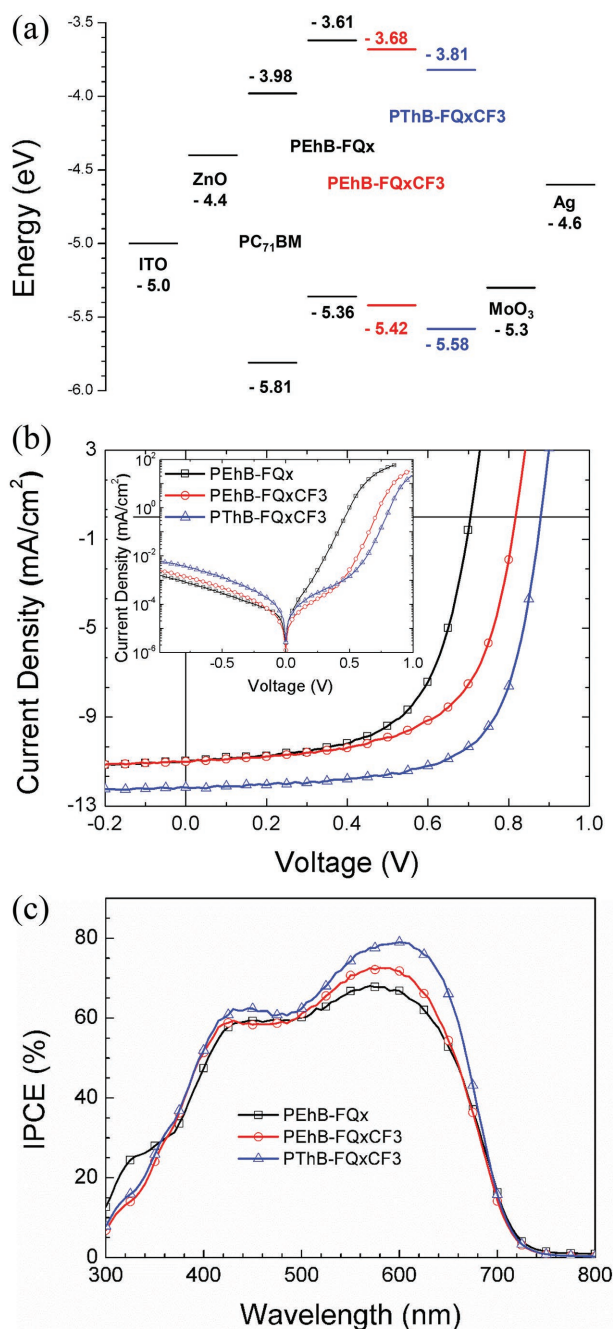


Figure 3. a) Energy level diagram of the materials in the inverted type PSCs, b) current density-voltage (J - V) curves of the PSCs, and c) IPCE spectra of the PSCs based on PEhB-FQx, PEhB-FQxCF₃, and PThB-FQxCF₃.

Figure 3b displays the current density–voltage (J - V) curves of the PSCs with the optimum blend ratios of the polymeric donors to PC₇₁BM showing the best PCE under 1.0 sun condition (inset: under dark condition). The PCE of the device with PEhB-FQx as the reference polymer is limited to 4.80%, but dramatic improvements are observed in the devices based on PEhB-FQxCF₃ (5.59%) and PThB-FQxCF₃ (7.26%). Noticeably, the V_{oc} values of the devices with PEhB-FQxCF₃ and PThB-FQxCF₃ are as high as 0.82 V and 0.88 V, respectively,

Table 2. Summary of the best photovoltaic parameters of the PSCs. The average values of the parameters for each device are given in parentheses.

Polymer	J_{sc} [mA cm^{-2}]	V_{oc} [V]	FF [%]	PCE [%]	R_s [Ωcm^2] ^{a)}
PEhB-FQx	11.1 (10.9 \pm 0.14)	0.68 (0.68 \pm 0.00)	63.5 (63.0 \pm 0.96)	4.80 (4.68 \pm 0.96)	3.31
PEhB-FQxCF3	11.0 (10.5 \pm 0.36)	0.82 (0.82 \pm 0.00)	61.9 (63.1 \pm 0.85)	5.59 (5.43 \pm 0.15)	3.63
PThB-FQxCF3	12.2 (12.1 \pm 0.04)	0.88 (0.88 \pm 0.00)	67.8 (68.0 \pm 0.20)	7.26 (7.26 \pm 0.00)	2.31

^{a)}Series resistance is estimated from the corresponding best device.

representing an increase of 20.60% and 29.41%, respectively, over that of the PEhB-FQx-based PSC (0.68%). The sharp increases in V_{oc} agree well with the deeper HOMO energy levels of PEhB-FQxCF3 and PThB-FQxCF3 (vide supra). The device based on PThB-FQxCF3 displays the best value of the short-circuit current (J_{sc}) at 12.20 mA cm^{-2} , compared to the devices adopting PEhB-FQx (11.10 mA cm^{-2}) and PEhB-FQxCF3 (11.00 mA cm^{-2}). Similarly, the fill factor (FF) of the device with PThB-FQxCF3 is the highest at 67.80%, while those of the devices based on PEhB-FQx and PEhB-FQxCF3 are limited to 63.50% and 61.90%, respectively. All the photovoltaic parameters of the devices with PEhB-FQx, PEhB-FQxCF3, and PThB-FQxCF3 are summarized in **Table 2**. As seen in Figure 3c, the incident photon-to-current efficiency (IPCE) curves of all the devices show good responses in the range 300–700 nm. In addition, the series resistance (R_s) and shunt resistance (R_{sh}) data are obtained from the J - V curves under dark condition (inset of Figure 3b). The R_s of the device based on PThB-FQxCF3 is 2.31 Ωcm^2 , which is smaller than those of the device based on PEhB-FQx (3.31 Ωcm^2) and PEhB-FQxCF3 (3.63 Ωcm^2). On the other hand, the R_{sh} of the device adopting PThB-FQxCF3 (1.42 $\text{k}\Omega \text{cm}^2$) was larger than that of the device with PEhB-

FQxCF3 (0.72 $\text{k}\Omega \text{cm}^2$). The trends in the R_s and R_{sh} data agree well with the photovoltaic performances of the polymers.

Hole- and electron-only devices with structures of ITO/PEDOT:PSS (35 nm)/polymer:PC₇₁BM (\approx 90 nm)/Au (50 nm) and ITO/ZnO (15 nm)/polymer:PC₇₁BM (80 nm)/Al (100 nm), respectively, were fabricated and tested to investigate the charge transporting properties of the polymers. As shown in Figure S3a,b, Supporting Information, the J - V curves of all the polymers exhibit a characteristic space charge limited current (SCLC), which can be fitted well by the Mott–Gurney law.^[31] The hole mobilities of the devices based on PEhB-FQx, PEhB-FQxCF3, and PThB-FQxCF3 are 1.31×10^{-3} , 1.21×10^{-3} and $1.58 \times 10^{-3} \text{ cm}^2 \text{ V}^{-1} \text{ s}^{-1}$, respectively, while their electron mobilities are 1.02×10^{-3} , 1.47×10^{-3} and $1.90 \times 10^{-3} \text{ cm}^2 \text{ V}^{-1} \text{ s}^{-1}$, respectively. The hole and electron mobilities of PThB-FQxCF3 are higher than those of PEhB-FQx and PEhB-FQxCF3. This is another reason for the better performance of the device adopting PThB-FQxCF3.

The morphologies of the PEhB-FQx, PEhB-FQxCF3, and PThB-FQxCF3 films, and their blend films with PC₇₁BM, derived from transmission electron microscopy (TEM), are shown in **Figure 4**. The insets represent the corresponding selected-area electron diffraction (SAED) patterns. The films

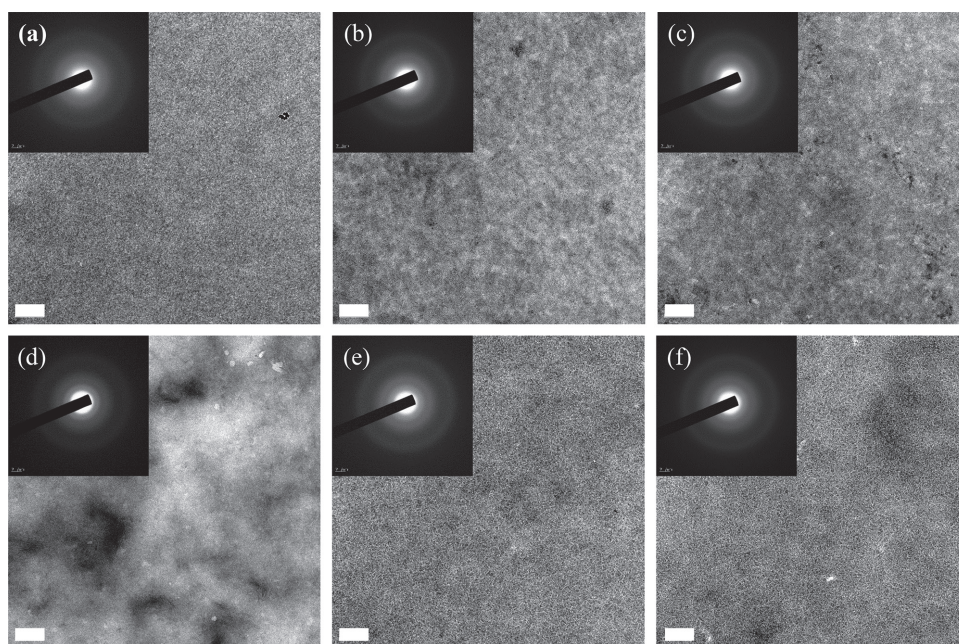


Figure 4. TEM images and (inset) the corresponding selected-area electron diffraction pattern (SAED) patterns of a) PEhB-FQx, b) PEhB-FQxCF3, c) PThB-FQxCF3, d) PEhB-FQx:PC₇₁BM (3:3), e) PEhB-FQxCF3:PC₇₁BM (3:4), and f) PThB-FQxCF3:PC₇₁BM (3:4). The scale bar is 0.2 μm .

of PEhB-FQx, PEhB-FQxCF₃, and PThB-FQxCF₃ exhibit relatively uniform morphologies with no distinct diffraction rings (Figure 4a–c). Meanwhile, a little larger phase separation and aggregation are observed from the blends based on PEhB-FQx and PEhB-FQxCF₃, while better nanoscale phase separation and bicontinuous interpenetrating networks can be formed in the blend based on PThB-FQxCF₃ (Figure 4d–f). In addition, the SAED images of blend films also exhibit unclear diffraction patterns only with the broad Debye–Scherrer diffraction rings originating from PC₇₁BM nanocrystals randomly distributed in PC₇₁BM-rich domains.^[32,33] Therefore, the formation of favorable nanoscale phase separation in the blend film of PThB-FQxCF₃ with PC₇₁BM can support the higher J_{sc} and FF of the related PSC through efficient charge separation and transport.^[34] Moreover, the tapping mode atomic force microscopy (AFM) measurements were conducted (Figure S4, Supporting Information) and the root-mean-square values of the blend based on PEhB-FQx:PC₇₁BM, PEhB-FQxCF₃:PC₇₁BM, and PThB-FQxCF₃:PC₇₁BM, are 3.52, 2.61, and 1.56 nm, respectively, indicating that surface roughness also affect the performance of the PSCs.

In this article, three conjugated polymers comprising electron-donating BDT and electron-accepting DFQ derivatives, denoted as PEhB-FQx, PEhB-FQxCF₃, and PThB-FQxCF₃, were designed and synthesized. The strong electron-withdrawing CF₃ group was introduced into the specific position of the DFQ unit of the reference polymer PEhB-FQx, to afford PEhB-FQxCF₃. In addition, the 2-ethylhexyloxy substituted group on the electron-donating BDT unit of PEhB-FQxCF₃ was replaced with 2-ethylhexyl thiophene moiety to produce PThB-FQxCF₃. An analysis of the resultant photovoltaic cells demonstrates that the PCEs of the devices gradually increased in the following order: PEhB-FQx (4.80%), PEhB-FQxCF₃ (5.59%), and PThB-FQxCF₃ (7.26%). The enhancement of PCE from PEhB-FQx to PEhB-FQxCF₃ can be attributed to the positive impact of the CF₃ substituents in the polymer backbone such as increase in V_{oc} by reduction in HOMO energy levels. Further improvement in PCE from PEhB-FQxCF₃ to PThB-FQxCF₃ was achieved through promotion of intermolecular coplanarity caused by introducing a thiophene ring on the BDT unit. This is also due to increase in V_{oc} with concomitant enhancement in J_{sc} and FF. Thus, this study can provide meaningful insights into the molecular design as well as structure–property relationships of the D–A type of conjugated polymers with strong electron-withdrawing CF₃ substituted moieties in their backbones for application in various emerging fields of photovoltaic cells and field-effect transistors.

Experimental Section

Experimental details of material synthesis, characterization, device fabrication, and analysis are included in the Supporting Information.

Supporting Information

Supporting Information is available from the Wiley Online Library or from the author

Acknowledgements

S.K.P. and Y.H.K. contributed equally to this work. This research was supported by Korea Institute of Energy Technology Evaluation and Planning (KETEP-20153010140030), and National Research Foundation of Korea (NRF-2015R1D1A1A01057410).

Conflict of Interest

The authors declare no conflict of interest.

Keywords

6, 7-difluorinated quinoxaline, electron-withdrawing substituents, polymer solar cells

Received: April 4, 2018

Revised: May 16, 2018

Published online: July 4, 2018

- [1] G. Li, R. Zhu, Y. Yang, *Nat. Photonics* **2012**, *6*, 153.
- [2] Y. Huang, E. J. Kramer, A. J. Heeger, G. C. Bazan, *Chem. Rev.* **2014**, *114*, 7006.
- [3] Y. Liu, J. Zhao, Z. Li, C. Mu, W. Ma, H. Hu, K. Jiang, H. Lin, H. Ade, H. Yan, *Nat. Commun.* **2014**, *5*, 5293.
- [4] J. Zhao, Y. Li, G. Yang, K. Jiang, H. Lin, H. Ade, W. Ma, H. Yan, *Nat. Energy* **2016**, *1*, 15027.
- [5] J. You, L. Dou, K. Yoshimura, T. Kato, K. Ohya, T. Moriarty, K. Emery, C.-C. Chen, J. Gao, G. Li, *Nat. Commun.* **2013**, *4*, 1446.
- [6] X. Xu, Z. Li, Z. Wang, K. Li, K. Feng, Q. Peng, *Nano Energy* **2016**, *25*, 170.
- [7] Y. J. Cheng, S. H. Yang, C. S. Hsu, *Chem. Rev.* **2009**, *109*, 5868.
- [8] Y. Li, *Acc. Chem. Res.* **2012**, *45*, 723.
- [9] J. Chen, Y. Cao, *Acc. Chem. Res.* **2009**, *42*, 1709.
- [10] H. Yao, L. Ye, H. Zhang, S. Li, S. Zhang, J. Hou, *Chem. Rev.* **2016**, *116*, 7397.
- [11] A. C. Stuart, J. R. Tumbleston, H. Zhou, W. Li, S. Liu, H. Ade, W. You, *J. Am. Chem. Soc.* **2013**, *135*, 1806.
- [12] S. C. Price, A. C. Stuart, L. Yang, H. Zhou, W. You, *J. Am. Chem. Soc.* **2011**, *133*, 4625.
- [13] X.-P. Xu, Y. Li, M. M. Luo, Q. Peng, *Chin. Chem. Lett.* **2016**, *27*, 1241.
- [14] S. K. Putri, Y. H. Kim, D. R. Whang, M. S. Lee, J. H. Kim, D. W. Chang, *Org. Electron.* **2017**, *47*, 14.
- [15] J. Yuan, L. Qiu, Z. G. Zhang, Y. Li, Y. Chen, Y. Zou, *Nano Energy* **2016**, *30*, 312.
- [16] S. Xu, L. Feng, J. Yuan, Z.-G. Zhang, Y. Li, H. Peng, Y. Zou, *ACS Appl. Mater. Interfaces* **2017**, *9*, 18816.
- [17] Z. Zheng, O. M. Awartani, B. Gautam, D. Liu, Y. Qin, W. Li, A. Battaller, K. Gundogdu, H. Ade, J. Hou, *Adv. Mater.* **2017**, *29*, 160241.
- [18] Y. Huang, L. Huo, S. Zhang, X. Guo, C. C. Han, Y. Li, J. Hou, *Chem. Commun.* **2011**, *47*, 8904.
- [19] J. Y. Shim, T. Kim, J. Kim, J. Kim, I. Kim, J. Y. Kim, H. Suh, *Syn. Met.* **2015**, *205*, 112.
- [20] A. Casey, S. D. Dimitrov, P. Shakya-Tuladhar, Z. Fei, M. Nguyen, Y. Han, T. D. Anthopoulos, J. R. Durrant, M. Heeney, *Chem. Mater.* **2016**, *28*, 5110.
- [21] C. Hansch, A. Leo, R. Taft, *Chem. Rev.* **1991**, *91*, 165.
- [22] M. Murali, A. D. Rao, P. C. Ramamurthy, *RSC Adv.* **2014**, *4*, 44902.
- [23] B. Zhang, G. Chen, J. Xu, L. Hu, W. Yang, *New J. Chem.* **2016**, *40*, 402.

- [24] P. Deng, Z. Wu, K. Cao, Q. Zhang, B. Sun, S. R. Marder, *Polym. Chem.* **2013**, *4*, 5275.
- [25] J. Yuan, L. Qiu, Z. Zhang, Y. Li, Y. He, L. Jiang, Y. Zou, *Chem. Commun.* **2016**, *52*, 6881.
- [26] J. Hou, H. Y. Chen, S. Zhang, R. I. Chen, Y. Yang, Y. Wu, G. Li, *J. Am. Chem. Soc.* **2009**, *131*, 15586.
- [27] L. Huo, S. Zhang, X. Guo, F. Xu, Y. Li, J. Hou, *Angew. Chem. Int. Ed.* **2011**, *123*, 9871.
- [28] M. Wang, D. Ma, K. Shi, S. Shi, S. Chen, C. Huang, Z. Qiao, Z. G. Zhang, Y. Li, X. Li, *J. Mater. Chem. A* **2015**, *3*, 2802.
- [29] S. H. Liao, H. J. Jhuo, Y. S. Cheng, S. A. Chen, *Adv. Mater.* **2013**, *25*, 4766.
- [30] M. Frisch, G. Trucks, H. Schlegel, G. Scuseria, M. Robb, J. Cheeseman, G. Scalmani, V. Barone, B. Mennucci, G. Petersson, Gaussian 09, revision D. 01, Gaussian, Inc., Wallingford, CT **2009**.
- [31] A. Bagui, S. S. K. Iyer, *Org. Electron.* **2014**, *15*, 1387.
- [32] X. Yang, J. K. van Duren, R. A. Janssen, M. A. Michels, J. Loos, *Macromolecules* **2004**, *37*, 2151.
- [33] X. Yang, J. K. van Duren, M. T. Rispens, J. C. Hummelen, R. A. Janssen, M. A. Michels, J. Loos, *Adv. Mater.* **2004**, *16*, 802.
- [34] L. Ye, S. Zhang, W. Zhao, H. Yao, J. Hou, *Chem. Mater.* **2014**, *26*, 3603.